TÜBİTAK

Turkish Journal of Chemistry

http://journals.tubitak.gov.tr/chem/

Research Article

Turk J Chem
(2017) 41: 931 – 943

doi:10.3906/kim-1701-46

Naked eye and smartphone applicable detection of toxic mercury ions using fluorescent carbon nanodots

Burcu BAÇ[1], Rükan GENÇ[1,2,*]
[1]Department of Chemical Engineering, Mersin University, Çiftlikköy Campus, Yenişehir, Mersin, Turkey
[2]Advanced Technology Education, Research, and Application Center (MEITAM), Mersin University, Çiftlikköy Campus, Yenişehir, Mersin, Turkey

Received: 19.01.2017 • **Accepted/Published Online:** 07.06.2017 • **Final Version:** 20.12.2017

Abstract: Chitosan passivated carbon nanodots (C-Dots$_{CHIT}$) were synthesized from expired molasses via a simple and green thermal synthesis procedure. As-synthesized C-Dots were nitrogen-doped (NC-Dots$_{CHIT}$) by posttreatment with liquid ammonia and used as nanoprobes for fluorometric detection of mercury ions (Hg(II)$_{aq.}$). Fluorescence response of NC-Dots$_{CHIT}$ in the presence of mercury was evaluated and compared with that of the polyethylene glycol passivated C-Dots$_{PEG}$. This sensing strategy using NC-Dots$_{CHIT}$ displayed a wide linear working range from 1.25 μg/mL to 43.54 μg/mL with a detection limit of 1.41 μg/mL. The fluorescence of C-Dots$_{PEG}$ did not show any significant change upon mercury addition. Selectivity of as-synthesized NC-Dots$_{CHIT}$ to Hg(II)$_{aq.}$ was assessed by comparing the level of fluorescence quenching in the presence of four other divalent cations (cadmium(II), zinc(II), nickel(II), and copper(II)). Finally, synthesized nanoprobes were embedded into the cross-linked alginate hydrogels and test strips were formed on the FTO-coated glass. Images captured under a UV light source (λexc: 365 nm) were successfully processed by a smartphone application. Color codes generated by the app showed a close resemblance to the data gathered from fluorescence spectroscopy. The proposed detection system was applied satisfactorily to both a certified calibration standard and real water samples. The methodology developed within this study could be a potential candidate for detection of mercury concentration in water samples with high recovery rates reaching up to 98%. This smartphone applicable detection platform that uses carbon nanodots as cheap yet sensitive nanoprobes could lead to more advanced lab-on-site systems for water or food sample analysis that can be performed by anyone, anywhere, anytime.

Key words: Mercury sensing, fluorescent carbon nanodots, nanoprobes, smartphone

1. Introduction

As a result of industrial developments accompanied by population growth, heavy metal pollution of the environment causes a significant threat to human health. It is well known that mercury is one of the most dangerous heavy metal types, which shows toxic effects even at low concentrations.[1] It is widely found as a constituent or contaminant in a variety of industrial processes, such as sodium hydroxide, chlorine, bleach (sodium hypochlorite) and caustic soda industry, batteries and battery chargers, gold mining, and the cement industry.[2–5] The most harmful form of the mercury ion is methyl mercury, which unfortunately causes neurological damage and other severe health problems along with detrimental effects on the environment.[1] Many analytical techniques, such as atomic absorption spectroscopy, chromatography, X-ray photoelectron spectroscopy, and inductively

*Correspondence: rukangnc@gmail.com

coupled plasma-mass spectrometry (ICP-MS), have been applied to monitor the presence of heavy metals in a wide range of samples.[6] However, detection of heavy metals with those devices is neither economic nor time-efficient.[7]

Various bio/chemosensors have been developed to provide mercury sensing with increased sensitivity and selectivity together with low fabrication cost.[8–10] Among these, colorimetric and fluorometric methods have been successfully applied for real-time mercury detection.[6,10–13] Inorganic quantum dots (QDots) are fluorescence-bearing nanoparticles that have often been used as a detection tool for many inorganic and organic substances.[14–17] The detection mechanism of QDot-based fluorescent sensors mainly requires fluorescent enhancement or quenching due to the physical or chemical attraction of the target to probe surface.[18,19] QDots have many important features including size-dependent photoluminescence, high quantum yield (QY), photoresistance, and nonblinking fluorescence emission. However, their use in sensors is limited by their intrinsic toxicity together with the laborious, time-consuming, and expensive synthesis procedures.[20] There are several attempts in the literature focused on the synthesis of less toxic and more effective nanoprobes, most of which use noble metals that are expensive and not stable for long term storage.[21]

Carbon nanodots (C-Dots), on the other hand, are environmentally friendly carbon-based materials in spherical form with graphene-like structural properties. They have optical properties that make them very promising alternatives to the conventional QDs. These include high fluorescence quantum yield equivalent to quantum dots, wavelength-dependent photoluminescence (PL) behavior, upconversion (fluorescence enhancement) fluorescence emission, and phosphorescence.[22–25] Recently, several studies highlighted the prospect of using fluorescent C-Dots in optochemical applications such as photovoltaic devices, light-emitting diodes, bioimaging/tracking, and sensor applications due to these features.[22,26–28] However, the most prominent feature of C-Dots as opposed to other carbonaceous nanomaterials and semiconducting QDs is that they can be synthesized directly by heating readily available natural carbon sources (fruit extracts, food waste, expired beverages, plant pods, etc.) without the need for time-consuming procedures and hazardous chemicals.[29–33] There are several recent reports on the use of C-Dots for monitoring heavy metals including tin (Sn)[34] copper[35] and mercury.[36] Wang et al. recently showed that NC-Dots$_{CHIT}$ from a presynthesized hydrosoluble chitosan have high selectivity to mercury ions.[37]

Mobile phone applicable systems open new venues for the development of portable analysis systems that provide on-site analysis of samples along with the possibility to store and share the analyzed data anytime with anyone.[38] Applications of smartphone technologies to colorimetric detection of many diseases[39,40], small molecules,[41] and toxins including heavy metals[42–44] have been reported by various groups, but there is still room for new detection strategies in this research field.

In this study, we report a cheap, nontoxic, high quantum yield fluorescent C-Dot-based nanoprobe produced from expired molasses for mercury ion detection. A postdoping step was performed to synthesize N-doped C-Dots. The selectivity and sensitivity of the resulting nanoprobes to Hg(II)$_{aq.}$ were evaluated by measuring the level of fluorescence quenching, and they were compared with polyethylene glycol passivated carbon nanodots (C-Dots$_{PEG}$). C-Dots were subjected to a mercury test strip by embedding them into the alginate hydrogels formed on the FTO-coated glass surface. Fluorescence images were then processed by a free smartphone app to evaluate the applicability of the developed system to lab-on-site detection systems.

2. Results and discussion

In a recent study, our group synthesized carbon nanodots using several macromolecules mixed with molasses through a one-step thermal synthesis method. Carbon nanodots passivated with polyethylene glycol and chitosan showed the highest QY values of 14.85% and 13.64%, respectively, in respect to other passivating agents used.[45] Here, we treated C-Dots$_{CHIT}$ with ammonia ($NH_{3(aq.)}$) (Scheme).[46] N-Doped nanoparticles exhibited an enhanced QY (17.80%) as compared with that of undoped C-Dots$_{CHIT}$ (13.64%) and C-Dots$_{PEG}$ (14.85%).

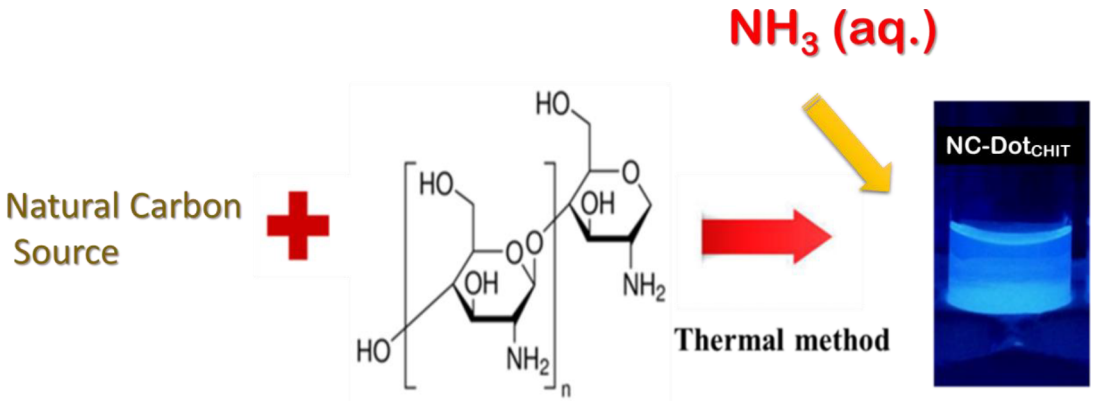

Scheme. Schematic representation of fluorescent C-Dot synthesis, postdoping of nanoparticles, and a digital image of NC-Dots$_{CHIT}$ under UV-light (λexc: 365 nm) irradiation.

Dynamic light scattering (DLS) measurements showed that postdoped C-Dots$_{@Chit}$ have a hydrodynamic radius of 15.4 $\pm$ 3.1 nm along with a polydispersity index of 0.231 (Figure 1). A polydispersity index below 0.5 indicates that synthesized nanoparticles are homogeneously dispersed and have narrow size distribution. As can be seen in the transmission electron microscopy (TEM) images of C-Dots$_{@Chit}$ depicted in Figure 1, the nanoparticles have a size below 10 nm, which is a little smaller than that measured by DLS. After the ammonia posttreatment, the zeta potential value of C-Dots$_{@Chit}$ decreased from –28.6 mV to –22.0 mV. This change indicates the presence of N-groups on the nanoparticle surface.

Polyethylene glycol (PEG) is often used as a passivating agent to enhance the fluorescence properties of C-Dots.[47] As depicted in Figures 2a and 2b, the addition of mercury ions over a wide concentration range of 0–87 μg/mL to C-Dots$_{@PEG}$ in solution did not change the fluorescence emission of the nanoparticles. Doped C-Dots$_{@Chit}$, on the other hand, gave a quick response to Hg(II)$_{aq.}$ and the fluorescence intensity of the sample quenched instantly (Figure 2c). Figure 2d shows that the fluorescence response of C-Dots$_{@Chit}$ was inversely proportional to mercury concentration. The assay showed good linearity between 1.25 and 43.54 μg/mL The regression equation is y = 0.008x + 1.0240 (R^2 = 0.983) and the limit of detection (LOD) was 1.41 μg/mL (S / N = 3). The comparison of detection range and LOD values of different detection systems is summarized in Table 1, indicating that the as-prepared C-Dots with detection limits reaching to μM levels can be used effectively as nanoprobes in fluorometric chemosensor development for mercury detection.[9,37,48–50]

Taking account that Hg(II)$_{aq.}$ is a divalent cation, the attraction of the mercury ions to the negative groups located on the nanoparticle surface by ionic interaction is likely. Upon addition of Hg(II)$_{aq.}$, the availability of electron transferring and oxygen bearing surface functional groups is expected to decrease, and, as a result, contact-induced fluorescence quenching should occur (Figures 2c and 2d). In order to see the effect

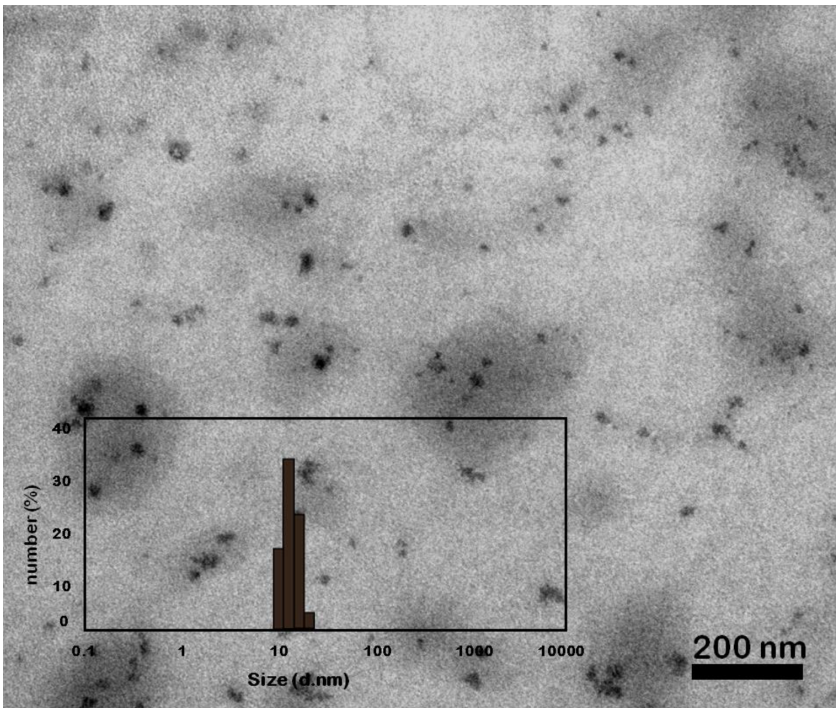

Figure 1. Size distribution graph by DLS and transmission electron image of water soluble NC-Dots$_{CHIT}$.

Table 1. Comparison of the results of the test system reported here with the literature.

Probe	Detection method	Regression line	LOD	Ref.
Ruthenium(II) dye	Colorimetric/luminescence sensor	4.23 μM to 0.423 M	0.4 μM	[9]
N-, S-, Co-doped C-Dots	Luminescence sensor	0–20 μM	0.18 μM	[37]
Triethanolamine-capped CdSe QDot	Fluorescent sensors	0 - 30 μM	19 μM	[48]
Unmodified gold nanoparticles	Aptamer-based colorimetric detection	10 nM to 0.1 mM	0.6 nM	[49]
Riboflavin-gold nanoparticles	Colorimetric	0.02–0.80?μM	14 nM	[50]
N-doped C-Dots$_{CHIT}$	Colorimetric/luminescence sensor	1.25–43.5 μg/mL	1.41 μg/mL	This study

of Hg(II) binding to the C-Dot surface, zeta potential measurements were conducted. Following the addition of Hg(II)$_{aq.}$ (87 μg/mL), the ζ-pot of the C-Dots$_{@Chit}$ dropped from 22.0 mV to –3.12 mV. However, only a slight change from –24.7 mV to –22.4 mV was observed in the case of C-Dots$_{@PEG}$. PEG with a large chain forms a very densely packed adsorption layer on the nanoparticle surface.[51] The diminished ionic interaction between the negative particle surface and mercury ion could be due to this protective layer that pushes the mercury out. The Fourier transform infrared (FTIR) spectrum of chitosan bearing C-Dots before and after addition of 87 μg/mL Hg(II)$_{aq.}$ revealed that both the oxygen bearing functional groups present on the surface (absorption bands at 1000–1200 cm^{-1}) and the amine III C-N bond peaks that appeared at 1570 cm^{-1} (Figure 3a) disappeared after surface interaction with mercury. Taken together, these results indicate that ionic forces

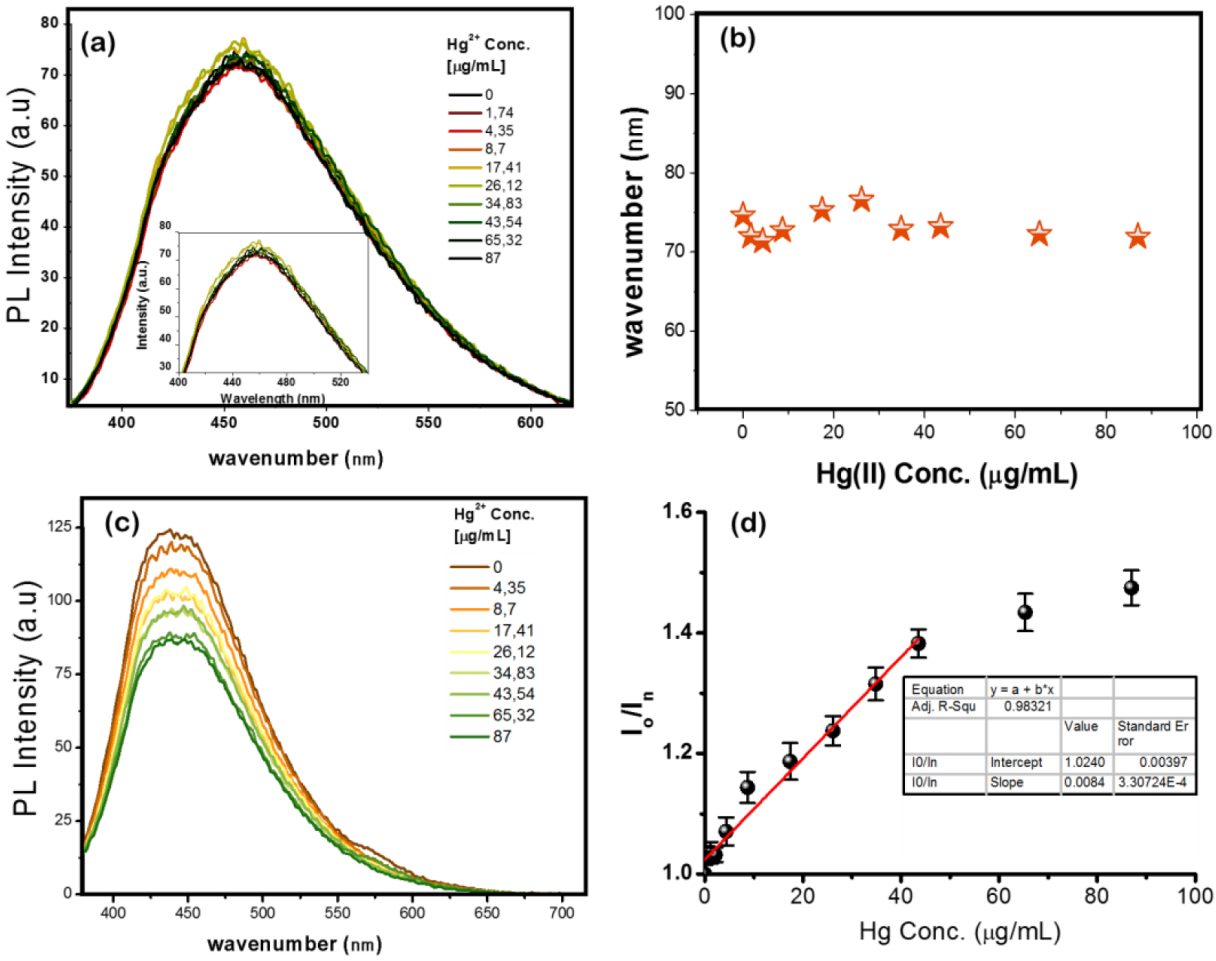

Figure 2. Fluorescence response of a, b) C-Dots$_{PEG}$ and c, d) NC-Dots$_{CHIT}$ against different concentrations of Hg(II)$_{aq}$.

and the binding sites that formed due to C-N groups have a synergetic effect on nanoprobe sensitivity and fluorescence quenching (Figures 3b and 3c).[52]

Selectivity of NC-Dots$_{@Chit}$ to mercury ions was further evaluated by comparing the fluorescence change in the presence of aqueous solutions (87 μg/mL) of various divalent heavy metals: Ni(II) (Mw = 58.69), Cd(II) (Mw = 112.4), Zn(II) (Mw = 65.38), Cu(II) (Mw = 63.50), and Hg(II) (Mw = 200.0). As can be seen from Figure 4a, the highest fluorescence loss was observed for mercury, while the fluorescence quenching in the presence of cadmium ions was negligible (Figures 4b and 4c). A gradual decrease in fluorescence was also observed for the rest of the ions but at a much lower magnitude than mercury. The low selectivity of the nanoprobe to Hg(II)$_{aq.}$ was due to electrostatic interaction of the divalent cations with the C-Dot surface. Thus, our ongoing studies are focused on tailoring the nanoparticle surface against nonspecific ionic interactions by neutralization of the negative charge on the particle surface and functionalization with thiocyanate (SCN^-) bearing polymers that specifically bind to mercury ions[53]

Finally, NC-Dots$_{@Chit}$ were subjected to a fluorine-doped tin oxide (FTO)-based glass test strip as nanoprobes by encapsulating them in an alginate hydrogel (0.5 $\times$ 0.5 cm) (Figure 5a). As presented in Figure 5b, NC-Dots$_{@Chit}$ -alginate hydrogel exhibits bright blue fluorescence when irradiated with UV light at 365

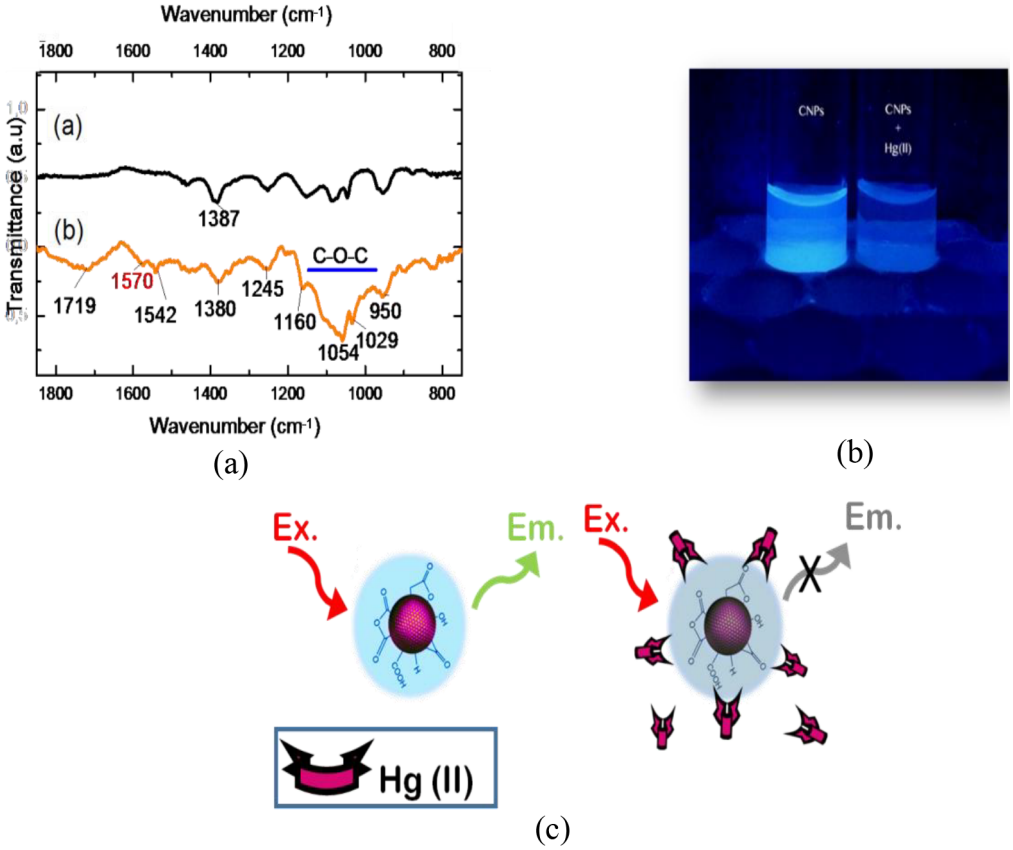

Figure 3. a) FTIR spectrum and b) fluorescence image (Ex. 365 nm) of NC-Dots$_{CHIT}$ before and after addition of 87 μg/mL of Hg(II)$_{aq.}$, and c) schematic representation of the fluorescence quenching as a result of surface interaction with mercury ions.

nm. Immediately after addition of a drop of 87 μg/mL Hg(II)$_{aq}$. to the test strip, fluorescence disappeared (Figure 5b). To the best of our knowledge, this is the first example of a real-time testing system that consists of C-Dots embedded in thin films for heavy metal sensing. Both the test strips developed and the solution-based testing methodology reported here offer on-time analysis of mercury in liquid samples without the requirement of high-tech analytic systems by checking the fluorescence loss. A simple black lamp is enough to provide a "yes–no" type of response for naked eye detection of Hg(II)$_{aq.}$ in liquid samples.[54,55]

Another option for quantitative analysis of the data is testing the system with smartphone technology.[56] To do so, we converted the fluorescence images in Figure 4c to color coding with a free Android application (Color Detector by Mobilia), and results are represented in Table 2 and Figures 6a and 6b. The values of the B color code showed a higher resemblance to the data gathered from fluorescence spectrophotometry. We further applied the same approach to the test strips shown in Figure 5b. As can be seen clearly from the results shown in Table 2, changes in color upon the addition of the mercury-containing sample are clearly distinguishable by tracking the change in B value. This simple sensing platform could provide on-site test systems that allow any smartphone user to analyze test samples anywhere and anytime by simply evaluating the fluorescence images using a black light and a free mobile phone application that can convert colors to color codes.

In order to assure the quality of results for the determination of mercury, the method was evaluated by a certified calibration standard for mercury (Multi-element Calibration Standard Hg, Agilent) spiked to

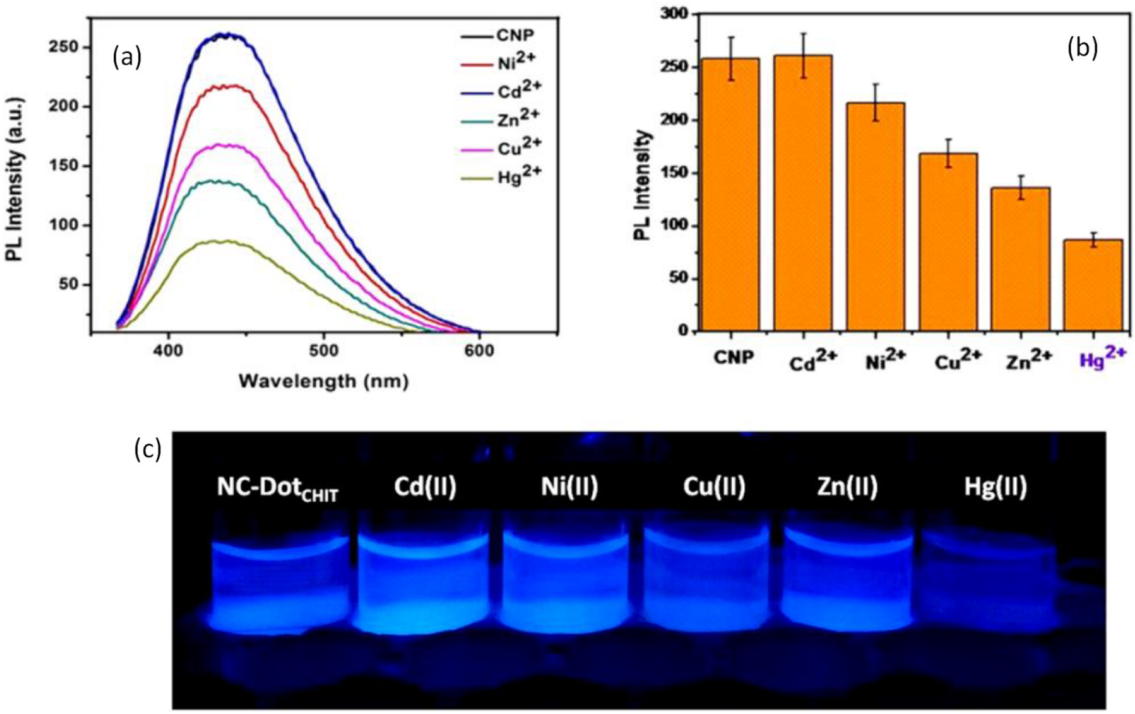

Figure 4. a, b) Fluorescence response of NC-Dots$_{CHIT}$ to different divalent heavy metal cations (87 μg/mL) and c) corresponding digital images at λexc: 365 nm.

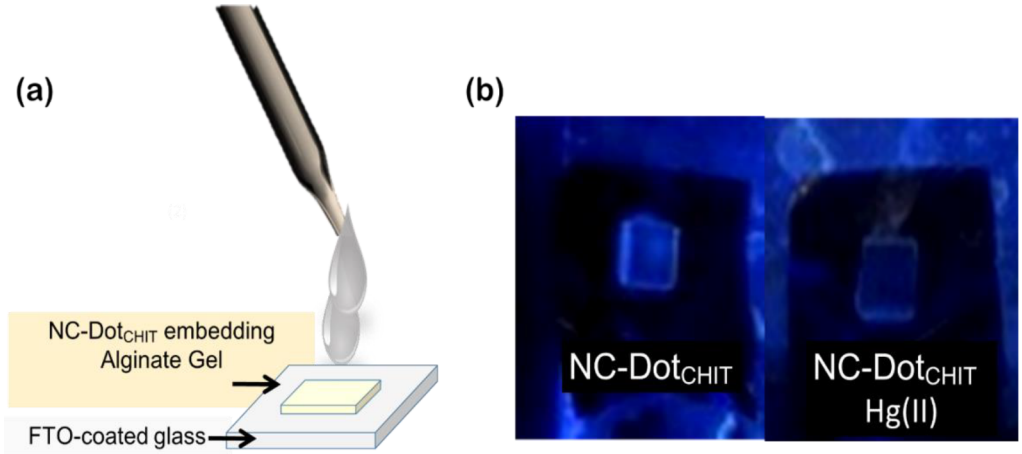

Figure 5. a) Construction of test strip and fluorescence image of b) before and after addition of 87 μg/mL of Hg(II)$_{aq.}$

obtain final mercury concentrations of 2.17, 4.35, and 8.7 μg/mL. Table 3 shows the mercury concentrations obtained by ICP-MS and the assay procedure reported here. The data show very good agreement with the certified values. Even at the lowest Hg concentration (2.17 μg/mL), an accurate determination of mercury with recovery rate higher than 95.8% was achieved. The recovery rate increased to 97.9% with increased mercury concentration (8.7 μg/mL).

Subsequently, the developed conditions were applied to three kinds of water samples (tap water, stream water, and sea water) posttreated with known concentrations of mercury: 8.7 μg/mL and 43.5 μg/mL. Water samples were analyzed both in solution and on the test strips and results were validated with the standard ICP-

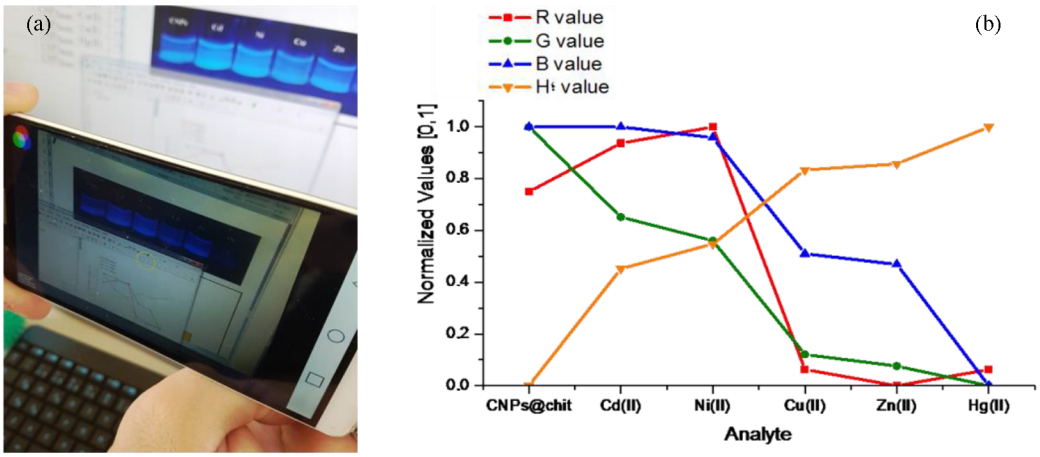

Figure 6. a) Mercury detection using a mobile phone application on digital images represented in Figure 4b, and b) the graph showing the corresponding RGB color codes and H° value.

Table 2. Color coding of fluorescence images depicted in Figure 4c and Figure 5b by a free Android application (Color Detector by Mobilia).

Test method	Analyte	HTML	R (%)	G- (%)	B- (%)	H° (%)
Dispersion	C-Dots$_{CHIT}$	#35c2fa	20	76	98	197
	C-Dots$_{CHIT}$ + Cd(II)$_{aq.}$	#3b88fc	23	53	98	216
	C-Dots$_{CHIT}$ + Ni(II)$_{aq.}$	#3e7ef6	24	47	96	220
	C-Dots$_{CHIT}$ + Cu(II)$_{aq.}$	#182fbd	9	18	74	232
	C-Dots$_{CHIT}$ + Zn(II)$_{aq.}$	#1527b9	8	15	72	233
	C-Dots$_{CHIT}$ + Hg(II)$_{aq.}$	#181a7e	9	10	49	239
Test strip	C-Dots$_{CHIT}$	#4a63e2	29	38	88	230
	C-Dots$_{CHIT}$ + Hg(II)$_{aq.}$	#26246d	14	14	42	242

Table 3. Analysis of certified calibration standard for mercury and real samples postcontaminated with mercury. Comparison of recovery rates using ICP-MS.

Analyte	Reference value (μg/mL)	ICP-MS (μg/mL ± SD)	Experimental value (μg/mL ± SD)	Recovery (%)
Calibration standard	2.17	2.17 ± 0.0008	2.25 ± 0.08	95.83
Calibration standard	4.35	4.34 ± 0.0011	4.49 ± 0.13	96.54
Calibration standard	8.7	8.69 ± 0.0017	8.86 ± 0.25	97.93
Tap water	8.7	8.65 ± 0.01	8.51 ± 0.41	98.38
Tap water	43.5	43.51 ± 0.02	41.4 ± 1.22	95.15
Stream water	8.7	8.66 ± 0.01	8.42 ± 0.34	97.23
Stream water	43.5	43.47 ± 0.02	41.9 ± 2.08	96.39
Sea water	8.7	8.65 ± 0.01	8.04 ± 0.61	92.95
Sea water	43.5	43.44 ± 0.03	40.91 ± 2.32	94.18

MS analysis procedure in order to evaluate the accuracy of the assay. The results are represented in Figure 7 and Table 3. High recovery rates reaching 98.4% and 97.2% with tap water and stream water, respectively, were achieved, while this value decreased to 92.9% for sea water (Figure 7a). The salt concentration was effective for decreased recovery. When the same study was conducted for the glass test strips, as can be clearly seen in Figure 7b, the fluorescence of the test strips was quenched immediately and this change was visible to the naked eye. These results indicated that the proposed detection method has potential in the quantitative and qualitative analysis of mercury ions in the presence of some coexisting substances.

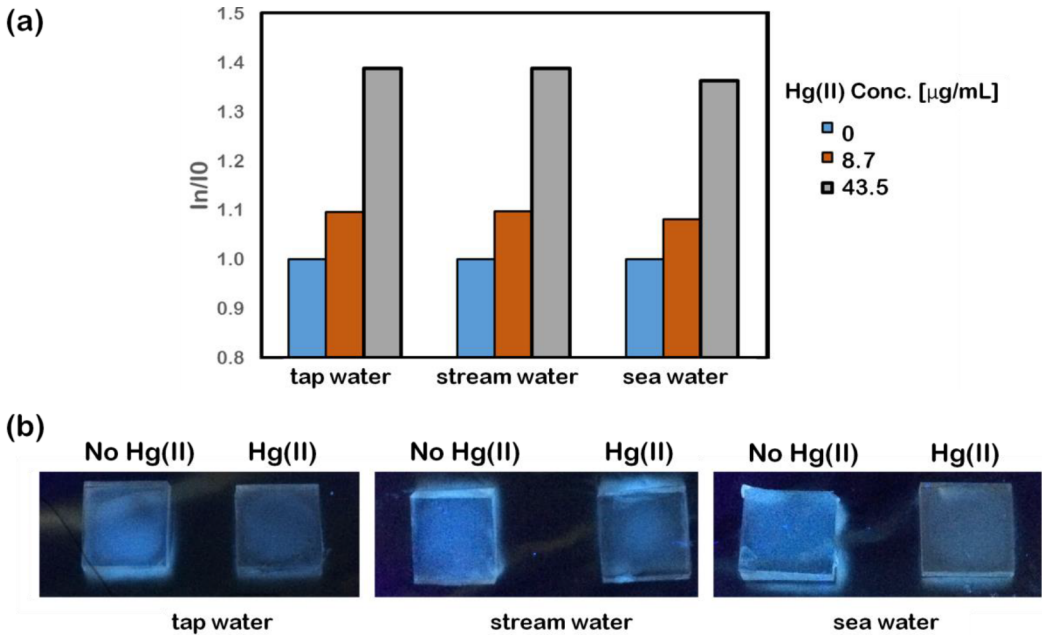

Figure 7. Studies with the real samples: a) fluorescence response of NC-DotsCHIT to the water samples contaminated with changing amounts of $Hg(II)_{aq.}$, and b) digital images showing the fluorescence quenching of test strips before and after the addition of water samples containing 43.5 μg/mL $Hg(II)_{aq}$.

In conclusion, a N-doped carbon nanodot ($NC\text{-}Dots_{CHIT}$)-based fluorometric and colorimetric assay for the detection of mercury (Hg) contamination in aqueous samples that can be applied to smartphone technology was reported here. The linear detection range of this water-soluble high quantum yield nanoprobe for Hg(II) was 1.25–43.5 μg/mL and the LOD was 1.41 μg/mL. The level of fluorescence quenching of C-Dots as a response to mercury ions was related to both the presence of N-groups and negatively charged surface functional groups presented on the nanoparticle surface. Selectivity of the produced C-Dots and the level of nonspecific interferences in the presence of other divalent heavy metals were also affected by particle surface properties. Moreover, with the incorporation of $NC\text{-}Dots_{CHIT}$ to hydrogel-based glass test strips, a "YES/NO" test for $Hg(II)_{aq.}$ in solution was demonstrated and observed by naked eye using a UV light source (λexc 365 nm) along with smartphone technology. The developed system was successfully applied to both a certified calibration reference solution and real water samples, which revealed a recovery level as high as 98%. Use of C-Dots as nanoprobes could be a very convenient approach for fluorescence-based heavy metal tests that can be performed by anyone without the need of professional personnel, anywhere and anytime.

3. Experimental

3.1. Materials

Poly(ethylene glycol) (PEG, Mn: 10KN) (CAS Number 25322-68-3), low molecular weight chitosan (50–190 kDa) (CAS Number: 9012-76-4), sodium alginate (CAS Number: 9005-38-3), calcium chloride salt, ammonium hydroxide solution, mercury(II) chloride, cadmium(II) chloride, zinc(II) chloride, nickel(II) chloride, and copper(II) chloride were purchased from Sigma-Aldrich. Certified standard solutions for mercury were prepared from a multielement calibration standard (10 mg/mL Hg, Agilent) manufactured under a UL ISO 900 quality assurance system provided by the Advanced Technology Education, Research, and Application Center (MEITAM) of Mersin University. Ethanol (96% pure grad.) was purchased from Fluka, carob molasses was purchased from a local grocery store, and the water used during synthesis was purified using a Millipore Milli-Q system (18.2 MQ-cm).

3.2. Instruments

DLS equipment (Zeta Sizer, Malvern NanoZS), FTIR spectroscopy (PerkinElmer Frontier, Waltham, MA, USA), Spectrum GX spectrometry within a range of 400–2000 cm^{-1}, TEM (JEOL), a Varian Cary Eclipse fluorescence spectrophotometer, a Milli-Q Reference Water Purification System, and an inductively coupled plasma mass spectrometer (Agilent 7500ce ICP-MS) (Agilent, Santa Clara, CA, USA) were used to characterize and evaluate the designed system.

3.3. Synthesis of C-Dots

FC-Dots were prepared by thermal synthesis.[33,57] One gram of commercial carob molasses was diluted in a 1:10 ratio in Milli-Q water (Ω = 18 MΩ cm) and 1 mL of this solution was then mixed with passivating agents (1:8 w:w) (PEG (10KN) and chitosan dispersed in 2 mL of 1:1 water/ethanol. The mixture was poured into a Teflon oven vessel after vigorous mixing. The mixture was maintained at 250 °C for 45 min. The resulting blackish material was dissolved in 2 mL of water. C-$Dots_{CHIT}$ were treated with 1 mL of ammonium hydroxide solution (10% v/v) and aged overnight under dark conditions. The obtained suspension was centrifuged at 5000 rpm for 30 min, and the supernatant was collected and vacuum-dried at 60 °C.

3.4. Characterization of C-Dots

The obtained water dispersible C-Dots were characterized by DLS and FTIR analysis. TEM was used to determine the size and morphology of the dispersed C-Dots. Photoluminescence of particle solutions was evaluated by fluorescence spectrophotometer. The QY of each sample was calculated taking quinine sulfate in 0.1 M H_2SO_4 as a reference fluorophore having a QY of 0.54% (λexc. 360 nm), following the procedure reported by Hemerson et al.[58]

3.5. Mercury(II) sensing and sensitivity evaluations

An FCNP solution (2.5 mg/mL) was prepared in Milli-Q water. The fluorescence measurements were carried out after each addition of $Hg(II)_{aq.}$ (100 mM) at microliter range (2 μL/each) to 3 mL of C-Dots in a quartz cuvette. Sensitivity testing was conducted following the same procedure using divalent heavy metals (cadmium(II) chloride, zinc(II) chloride, nickel(II) chloride, and copper(II) chloride).

Results were normalized taking into account the dilution factor and reported as I_0/I_n versus $Hg(II)_{aq.}$, where I_0 is the fluorescence intensity of the C-Dots at the beginning and I_n is the fluorescence intensity of the sample. The LOD was calculated as the concentration that corresponded to the intercept value plus three times the standard deviation of the regression line.

3.6. Preparation of glass test strips

$C\text{-}Dots_{CHIT}$ and $NC\text{-}Dots_{CHIT}$ were mixed with 4% alginate prepared in distilled water. The mixture was homogenized by vortexing. A FTO covered glass slide was cut with a diamond blade (1 × 1 cm). Alginate hydrogel was dropped to prepare a thin coating on the FTO by doctor blading. The glass slide was soaked in 10 at.% $CaCl_2$ and the 0.5 × 0.5 gel was observed as a yellowish opaque layer in daylight. Fluorescence emission from the C-Dot embedding hydrogels was visualized with a UV light source (365 nm) before and after $mercury(II)_{aq.}$ addition (20 μL).

3.7. Data evaluation by mobile phone application

A free Android application (Color Detector by Mobilia) was used for color coding of fluorescence images and results were correlated with the fluorescence spectrophotometer results.

4. Real sample analysis and assay accuracy

In order to evaluate the as-developed system on real sample detection, tap water (from the lab), stream water (Müftü Stream, Mersin), and sea water (Mediterranean Sea, Mersin) samples were collected and filtered through filter paper. $HgCl_2$ (8.7 μg/mL, 43.5 μg/mL) solutions were prepared in sample water solutions to obtain the spiked samples. Meanwhile, accuracy of the assay was evaluated by using a certified standard for Hg prepared in Milli-Q water at final Hg concentrations of 2.17, 4.35, and 8.7 μg/mL. $Hg(II)_{aq.}$ detection in real samples was carried out using the procedure described in Sections 3.5 and 3.6. Validations were done with the standard ICP-MS procedure (http://www.usp.org) by diluting the samples 10 times with 5% HNO_3, and test recovery and accuracy were calculated by taking ICP-MS results as 100%. The dilution factor was taken into account in the final calculations ($n > 3$).

References

1. Zahir, F.; Rizwi, S. J.; Haq, S. K.; Khan, R. H. *Environ. Toxicol. Pharmacol.* **2005**, *20*, 351-360.
2. Stellman, J. M.; International Labour Office. *Encyclopaedia of Occupational Health and Safety.*; International Labour Office: Geneva, Switzerland, 1998.
3. Wang, F.; Wang, S.; Zhang, L.; Yang, H.; Wu, Q.; Hao, J. *J. Hazard. Mater.* **2016**, *302*, 27-35.
4. Eisler, R. *Rev. Environ. Contam. Toxicol.* **2004**, *181*, 139-198.
5. Nolan, M.; Tucker, I. *Scand. Audiol.* **1981**, *10*, 189-191.
6. Qi, Y. X.; Zhang, M.; Zhu, A.; Shi, G. *Analyst* **2015**, *140*, 5656-5661.
7. Jew, A. D.; Kim, C. S.; Rytuba, J. J.; Gustin, M. S.; Brown, G. E. *Environ. Sci. Technol.* **2011**, *45*, 412-417.
8. Zhang, Y.; Chen, H.; Chen, D.; Wu, D.; Chen, Z.; Zhang, J.; Chen, X.; Liu, S.; Yin, J. *Sensors Actuators B Chem.* **2016**, *224*, 907-914.
9. Fan, S. H.; Shen, J.; Wu, H.; Wang, K. Z.; Zhang, A. G. *Chinese Chem. Lett.* **2014**, *26*, 580-584.
10. Nazeeruddin, M. K.; Di Censo, D.; Humphry-Baker, R.; Grätzel, M. *Adv. Funct. Mater.* **2006**, *16*, 189-194.

11. Krejcova, L.; Dospivova, D.; Ryvolova, M.; Kopel, P.; Hynek, D.; Krizkova, S.; Hubalek, J.; Adam, V.; Kizek, R. *Electrophoresis* **2012**, *33*, 3195-3204.
12. Maity, D.; Kumar, A.; Gunupuru, R.; Paul, P. *Colloid. Surface. A* **2014**, *455*, 122-128.
13. Wu, G. W.; He, S. B.; Peng, H. P.; Deng, H. H.; Liu, A. L.; Lin, X. H.; Xia, X. H.; Chen, W. *Anal. Chem.* **2014**, *86*, 10955-10960.
14. Su, X. L.; Li, Y. *Anal. Chem.* **2004**, *76*, 4806-4810.
15. Wegner, K. D.; Lanh, P. T.; Jennings, T.; Oh, E.; Jain, V.; Fairclough, S. M.; Smith, J. M.; Giovanelli, E.; Lequeux, N.; Pons, T. et al. *ACS Appl. Mater. Interfaces* **2013**, *5*, 2881-2892.
16. Algar, W. R.; Malanoski, A. P.; Susumu, K.; Stewart, M. H.; Hildebrandt, N.; Medintz, I. L. *Anal. Chem.* **2012**, *84*, 10136-10146.
17. Gao, X.; Du, C.; Zhuang, Z.; Chen, W. *J. Mater. Chem. C* **2016**, *4*, 6927-6945.
18. Pérez-López, B.; Merkoçi, A. *Trends Food Sci. Technol.* **2011**, *22*, 625-639.
19. Genç, R. In *Nanobiosensors in Nanotechnology in the Food Industry, Multi Volume Book Series*; Grumezescu, A. M., Ed. Academic Press: New York, NY, USA, 2016, pp. 391-428.
20. Asokan, S.; Krueger, K. M.; Alkhawaldeh, A.; Carreon, A. R.; Mu, Z.; Colvin, V. L.; Mantzaris, N. V; Wong, M. S. *Nanotechnology* **2005**, *16*, 2000-2011.
21. Nolan, E. M.; Lippard, S. J. *Chem. Rev.* **2008**, *108*, 3443-3480.
22. Li, H.; Kang, Z.; Liu, Y.; Lee, S. T. *J. Mater. Chem.* **2012**, *22*, 24230.
23. Choi, Y.; Kim, S.; Choi, M. H.; Ryoo, S. R.; Park, J.; Min, D. H.; Kim, B. S. *Adv. Funct. Mater.* **2014**, *24*, 5781-5789.
24. Baker, S. N.; Baker, G. A. *Angew. Chemie Int. Ed.* **2010**, *49*, 6726-6744.
25. Yu, P.; Wen, X.; Toh, Y. R.; Lee, Y. C.; Huang, K. Y.; Huang, S.; Shrestha, S.; Conibeer, G.; Tang, J. *J. Mater. Chem. C* **2014**, *2*, 2894.
26. Baker, S. N.; Baker, G. A. *Angew. Chemie Int. Ed.* **2010**, *49*, 6726-6744.
27. Juzenas, P.; Kleinauskas, A.; George Luo, P.; Sun, Y. P. *Appl. Phys. Lett.* **2013**, *103*, 10-14.
28. Wang, J.; Zhang, Z.; Zha, S.; Zhu, Y.; Wu, P.; Ehrenberg, B.; Chen, J. Y. *Biomaterials* **2014**, *35*, 9372-9381.
29. Li, C. L.; Ou, C. M.; Huang, C. C.; Wu, W. C.; Chen, Y. P.; Lin, T. E.; Ho, L. C.; Wang, C. W.; Shih, C. C.; Zhou, H. C. et al. *J. Mater. Chem. B* **2014**, *2*, 4564-4571.
30. Ke, Y.; Garg, B.; Ling, Y. *RSC Adv.* **2014**, *4*, 58329-58336.
31. Wu, D.; Deng, X.; Huang, X.; Wang, K.; Liu, Q. *J. Nanosci. Nanotechnol.* **2013**, *13*, 6611-6616.
32. Lin, P. Y.; Hsieh, C. W.; Kung, M. L.; Chu, L. Y.; Huang, H. J.; Chen, H. T.; Wu, D. C.; Kuo, C. H.; Hsieh, S. L.; Hsieh, S. *J. Biotechnol.* **2014**, *189*, 114-119.
33. Alas, M. O.; Genç, R. *Sinop University Journal of Natural Sciences* **2016**, *1*, 123-139.
34. Mohd Yazid, S. N. A.; Chin, S. F.; Pang, S. C.; Ng, S. M. *Microchim. Acta* **2013**, *180*, 137-143.
35. Wang, Y.; Zhang, C.; Chen, X.; Yang, B.; Yang, L.; Jiang, C.; Zhang, Z.; Hu, Q.; Zhang, Z. *Nanoscale* **2016**, *8*, 5977-5984.
36. Lu, W.; Qin, X.; Liu, S.; Chang, G.; Zhang, Y.; Luo, Y.; Asiri, A. M.; Al-Youbi, A. O.; Sun, X. *Anal. Chem.* **2012**, *84*, 5351-5357.
37. Wang, Y.; Kim, S. H.; Feng, L. *Anal. Chim. Acta* **2015**, *890*, 134-142.
38. Kim, H.; Jung, Y.; Doh, I. J.; Lozano-Mahecha, R. A.; Applegate, B.; Bae, E. *Sci. Rep.* **2017**, *7*, 40203.
39. Wang, L. J.; Chang, Y. C.; Sun, R.; Li, L. *Biosens. Bioelectron.* **2017**, *87*, 686-692.
40. Nakhleh, M. K.; Amal, H.; Jeries, R.; Broza, Y. Y.; Aboud, M.; Gharra, A.; Ivgi, H.; Khatib, S.; Badarneh, S.; Har-Shai, L. et al. *ACS Nano* **2017**, *11*, 112-125.

41. Vobornikova, I.; Pohanka, M. *Neuroendocrinol. Lett.* **2016**, *37*, 139-143.
42. Yu, S.; Xiao, W.; Fu, Q.; Wu, Z.; Yao, C.; Shen, H.; Tang, Y.; Cunningham, B. T.; Wang, B.; Lu, S. Y. et al. *Anal. Methods* **2016**, *8*, 6877-6882.
43. Xiao, W.; Xiao, M.; Fu, Q.; Yu, S.; Shen, H.; Bian, H.; Tang, Y. *Sensors* **2016**, *16*, 1871.
44. Wei, Q.; Nagi, R.; Sadeghi, K.; Feng, S.; Yan, E.; Ki, S. J.; Caire, R.; Tseng, D.; Ozcan, A. *ACS Nano* **2014**, *8*, 1121-1129.
45. Alas, M. O.; Genç, R. *J. Nanoparticle Res.* **2017**, *19*, 185-200.
46. Kan-nari, N.; Okamura, S.; Fujita, S.; Ozaki, J.; Arai, M. *Adv. Synth. Catal.* **2010**, *352*, 1476-1484.
47. Hao, Y.; Gan, Z.; Xu, J.; Wu, X.; Chu, P. K. *Appl. Surf. Sci.* **2014**, *311*, 490-497.
48. Shang, Z. Bin; Wang, Y.; Jin, W. J. *Talanta* **2009**, *78*, 364-369.
49. Li, L.; Li, B.; Qi, Y.; Jin, Y. *Anal. Bioanal. Chem.* **2009**, *393*, 2051-2057.
50. Xu, D.; Zhao, H. W.; Huang, C. Z.; Wu, L. P.; Pu, W. D.; Zheng, J. J.; Zuo, Y. *J. Nanosci. Nanotechnol.* **2012**, *12*, 3006-3010.
51. Ostolska, I.; Wiśniewska, M. *Colloid Polym. Sci.* **2014**, *292*, 2453-2464.
52. Yan, Z.; Yuen, M. F.; Hu, L.; Sun, P.; Lee, C. S. *RSC Adv.* **2014**, *4*, 48373-48388.
53. Hao, Y.; Xiong, D.; Wang, L.; Chen, W.; Zhou, B.; Liu, Y. N. *Talanta* **2013**, *115*, 253-257.
54. Sirawatcharin, S.; Saithongdee, A.; Chaicham, A.; Tomapatanaget, B.; Imyim, A.; Praphairaksit, N. *Anal. Sci.* **2014**, *30*, 1129-1134.
55. Kanayama, N.; Takarada, T.; Maeda, M. *Chem. Commun.* **2011**, *47*, 2077.
56. Jiang, J.; Wang, X.; Chao, R.; Ren, Y.; Hu, C.; Xu, Z.; Liu, G. L. *Sensor. Actuat. B-Chem.* **2014**, *193*, 653-659.
57. Mukherjee, P.; Misra, S. K.; Gryka, M. C.; Chang, H. H.; Tiwari, S.; Wilson, W. L.; Scott, J. W.; Bhargava, R.; Pan, D. *Small* **2015**, *11*, 4691-4703.
58. Castro, H. P. S.; Souza, V. S.; Scholten, J. D.; Dias, J. H.; Fernandes, J. A.; Rodembusch, F. S.; dos Reis, R.; Dupont, J.; Teixeira, S. R.; Correia, R. R. B. *Chem. A Eur. J.* **2016**, *22*, 138-143.